

Improved Detection Rates for Close Binaries Via Astrometric Observations of Gravitational Microlensing Events

Kyongae Chang
Department of Physics,
Chongju University, Chongju, Korea 360-764,
kchang@alpha94.chongju.ac.kr,

&

Cheongho Han
Department of Astronomy & Space Science,
Chungbuk National University, Chongju, Korea 361-763
cheongho@astronomy.chungbuk.ac.kr,

Received _____; accepted _____

ABSTRACT

In addition to constructing a Galactic matter mass function free from the bias induced by the hydrogen-burning limit, gravitational microlensing allows one to construct a mass function which is less affected by the problem of unresolved binaries (Gaudi & Gould). However, even with the method of microlensing, the photometric detection of binaries is limited to binary systems with relatively large separations of $b \gtrsim 0.4$ of their combined Einstein ring radius, and thus the mass function is still not totally free from the problem of unresolved binaries. In this paper, we show that by detecting distortions of the astrometric ellipse of a microlensing event with high precision instruments such as the *Space Interferometry Mission*, one can detect close binaries at a much higher rate than by the photometric method. We find that by astrometrically observing microlensing events, $\sim 50\%$ of binaries with separations of $0.1r_E$ can be detected with the detection threshold of 3% . The proposed astrometric method is especially efficient at detecting very close binaries. With a detection threshold of 3% and a rate of 10% , one can astrometrically detect binaries with separations down to $\sim 0.01r_E$.

Subject headings: binaries: visual – gravitational lensing – stars: mass function

submitted to *The Astrophysical Journal*: Jan 15, 1999

Preprint: CNU-A&SS-01/99

1. Introduction

Surveys to discover gravitational microlensing events have been and are being conducted toward the Galactic bulge and Magellanic Clouds (Alcock et al. 1997a, 1997b; Ansari et al. 1996; Udalski et al. 1997; Alard & Guibert 1997). The experiments are so successful that more than ~ 300 events have been detected. As the number of events increases, one can construct the mass function of lens matter (Han & Gould 1996; Zhao, Rich, & Spergel 1996; Gould, 1996; Han & Chang 1998). Since microlensing events can occur regardless of the lens brightness, the mass function constructed from the result of microlensing experiments is completely free from the bias induced by the lens brightness and can be extended down to very low mass stars and even brown dwarfs. By using new techniques of pixel method (Ansari et al. 1997) and image subtraction (Crotts 1992; Tomaney & Crotts 1996), the lensing experiments are extended toward unresolved star fields of M31.

Another important advantage of constructing a mass function with microlensing observations is that one can better control the problem of unresolved binaries. If one assumes that the individual masses measured are due to single objects without considering unresolved binaries, the constructed mass function will be biased toward larger masses (Reid 1991; Kroupa, Tout, & Gilmore 1991). With the conventional star count method, it is nearly impossible to resolve individual binary components, and thus the correction is achieved based on very uncertain models of the fraction of binaries and the mass ratios of their components. On the other hand, observations of microlensing events is an efficient method to detect binaries. If an event is caused by a binary lens, the resulting light curve differs from that of an event produced by a single-point lens. Therefore, by detecting the deviations of the light curve from the single-lens event light curve, one can detect binaries (Dominik 1998; Mao & Paczyński 1991). According to the microlensing detection rate for binaries computed by Gaudi & Gould (1997), a significant fraction of binary systems with separations greater than $b \sim 0.4$ of their combined Einstein ring radius, r_E , are detectable with a detection threshold of 3%.

However, even with the method of microlensing, the photometric detection of binary lenses is limited to binary systems with relatively large separations of $b \gtrsim 0.4$. The typical value of the Einstein ring radius for a Galactic bulge event is $r_E \sim 2$ AU for a lens mass of $1 M_\odot$. According to the model distribution of binary separations determined by Duquennoy & Mayor (1991, see also Figure 1 of Han & Jeong 1998), still a considerable fraction ($\sim 20\%$) of binary lenses have separations less than $b \sim 0.4r_E \sim 1$ AU. Therefore, although photometric observations of binary-lens events provides a superior method to conventional methods, the mass function constructed by this method cannot be totally free from the problem of unresolved binaries.

Recently, routine astrometric followup observations of microlensing events with high precision instruments such as the *Space Interferometry Mission* (hereafter SIM, <http://sim.jpl.nasa.gov>) are being discussed as a method to measure the distance and mass of a MACHO (Paczynski 1998; Boden, Shao, & Van Buren 1998). When a microlensing event is caused by a single-point lens, the observed source star image is split into two, and

the location of the center of light between the separate images with respect to the source star traces out an ellipse (astrometric ellipse; Walker 1995; Jeong, Han, & Park 1999). However, if the lens is composed of binaries, both the number and locations of images differ from those of a single-lens event, resulting in distorted astrometric ellipse (Safizadeh, Dalal, & Griest 1998).

In this paper, we show that by detecting the distortions of the astrometric ellipse, one can detect close binaries at a much higher rate than with the photometric method. We find that by astrometrically observing gravitational microlensing events, nearly half of binaries with separations of $0.1r_E$ can be detected with the detection threshold of 3%. The proposed astrometric method is especially efficient to detect very close binaries. With the detection threshold of 3% and a rate of 10%, one can astrometrically detect binaries with separations down to $\sim 0.01r_E$.

2. Very Close Binary Lens Events

When the lengths are normalized to the combined Einstein ring radius, the lens equation in complex notations for a binary lens system is given by

$$\zeta = z + \frac{m_1}{\bar{z}_1 - \bar{z}} + \frac{m_2}{\bar{z}_2 - \bar{z}}, \quad (2.1)$$

where m_1 and m_2 are the mass fractions of individual lenses (and thus $m_1 + m_2 = 1$), z_1 and z_2 are the positions of the lenses, $\zeta = \xi + i\eta$ and $z = x + iy$ are the positions of the source and images, and \bar{z} denotes the complex conjugate of z (Witt 1990). The combined Einstein ring radius is related to the lens parameters by

$$r_E = \left(\frac{4GM}{c^2} \frac{D_{ol}D_{ls}}{D_{os}} \right)^{1/2}, \quad (2.2)$$

where M is the total mass of the binary system, and D_{ol} , D_{ls} , and D_{os} are the distances between observer-lens, lens-source, and observer-source, respectively. The amplification of each image, A_i , is given by the Jacobian of the transformation (2.1) evaluated at the images position, i.e.,

$$A_i = \left(\frac{1}{|\det J|} \right)_{z=z_i}; \quad \det J = 1 - \frac{\partial \zeta}{\partial \bar{z}} \frac{\partial \bar{\zeta}}{\partial z}. \quad (2.3)$$

The images and source positions with infinite amplifications, i.e. $\det J = 0$, form closed curves, called critical curves and caustics, respectively. The positions of individual images are obtained by numerically solving equation (2.1). The amplification of a source star is given by the sum of the individual amplifications, $A = \sum_i A_i$, which are determined by equation (2.3).

Due to the presence of an additional lens object, the geometry of a binary-lens event differs from that of a single-lens event. In Figure 1, we present the geometry of gravitational

microlensing for various binary lens separations. In the figure, the two lenses (indicated by two dots on the ξ -axis) are assumed to have identical masses, i.e. $m_1 = m_2$, and the separation between them in units of the Einstein ring radius, b , is marked in each panel. The closed figures drawn with dotted and thick solid lines represent critical curves and caustics, respectively. For events with $b = 0.1$ and $b = 0.4$, there exist two additional triangular caustics outside the regions shown. In addition, there are two small circular critical curves near the diamond-shaped central caustic, but they are too small to be seen in the figure. The arclets drawn with a thin solid line represent the images of the source star, which is located at $(\xi, \eta) = (-0.3, -0.32)$ and is marked by an shaded circle. The source star is assumed to have a radius of $0.05r_E$. As the binary separation increases, the critical curve deviates from a circular Einstein ring and complex caustic structures form. When the source star is located outside the caustics as shown in the figure, there exist three images. In the figure, the smallest image inside the central caustic for small b is too small to be seen. On the other hand, when a source crosses a caustic, an extra pair of images appear or disappear, producing a sharp rise or drop in the light curve (Schneider & Weiss 1986).

However, if the separation between binary components is very small, the geometry of the binary-lens system mimics that of a single-lens system. In addition, the light curve imitates that of an event caused by a single-point lens with a mass equal to the total mass of the binary and located at the center of mass of the binary, making it difficult to photometrically distinguish the binary-lens event from a single-lens event. The light curve of a single-lens event is represented by

$$A_0 = \frac{u^2 + 2}{u(u^2 + 4)^{1/2}}, \quad u = \left[\beta^2 + \left(\frac{t - t_0}{t_E} \right)^2 \right]^{1/2}, \quad (2.4)$$

where u is the lens-source separation in units of the angular Einstein ring radius $\theta_E = r_E/D_{ol}$, β is the impact parameter of the lens-source encounter, t_0 is the time of maximum amplification, and t_E is the Einstein ring radius crossing time scale. If the position of the binary center of mass is at the origin, $u \equiv |\zeta|$. In the lower panel of Figure 2, we present light curves for the binary-lens events in the upper left panel of Figure 1, in which the corresponding source star trajectories are marked by straight lines. In the figure, the ‘x’ marks represent the amplifications for the binary-lens events, while the smooth solid curves are for the corresponding single-lens events. One finds that the light curves can be well approximated by those of single-lens events except those with very small impact parameters.

On the other hand, the difference in the astrometric shifts of source star image centroids ($\vec{\delta\theta}_c$, hereafter centroid shifts) between the binary-lens and the corresponding single-lens events is considerable compared to the difference in amplifications. In the upper panel of Figure 2, we present the centroid shifts of the binary-lens events (marked by ‘x’) for the same source star trajectories in the upper panel of Figure 1. For a single-mass lens event, the centroid shift is represented by

$$\vec{\delta\theta}_c = \frac{\theta_E}{u^2 + 2} (u_x \hat{\mathbf{x}} + u_y \hat{\mathbf{y}}), \quad (2.5)$$

where x and y represent the directions parallel and normal to the lens-source transverse motion, $u_x = (t - t_0)/t_E$ and $u_y = \beta$ are the two components of the lens-source separation vector \mathbf{u} (Walker 1995). For comparison of the centroid shifts between the binary-lens and corresponding single-lens events, we also present the trajectories of the expected centroid shifts of single-lens events, i.e. astrometric ellipses (smooth solid curves). For the computation of both the amplifications and centroid shifts, we assume a point source. One finds that the difference in the centroid shifts between the binary-lens and single-lens events are considerable even for events with large impact parameters.

3. Detection Rate for Close Binaries

In the previous section, we showed by examples that close binaries can be more easily detected astrometrically than by the photometric observations of microlensing events. In this section, we statistically compute the binary detection rate from the astrometric observations of binary lens events and compare it to the rate determined by the photometric method. For direct comparison of the astrometric detection rate, Γ_{ast} , to the photometric detection rate, Γ_{ph} , computed by Gaudi & Gould (1997), we adopt their method of analysis.

To analyze how the centroid shift and amplification of a binary-lens event deviates from a single-lens event, we define the excess centroid shift and amplification by

$$\epsilon_{\delta\theta_c} = \frac{|\vec{\delta\theta}_c - \vec{\delta\theta}_{c,0}|}{\delta\theta_{c,0}}, \quad (3.1)$$

and

$$\epsilon_A = \frac{A - A_0}{A_0}, \quad (3.2)$$

where $\vec{\delta\theta}_{c,0}$ is the centroid shift for a single-lens event. Since the centroid shift is a two-dimensional vector, we compute the excess centroid shifts based on the absolute value of the difference between $\vec{\delta\theta}_c$ and $\vec{\delta\theta}_{c,0}$, not on the subtraction of their scalar values. We then compute the values of $\epsilon_{\delta\theta_c}$ and ϵ_A as a function of source position, i.e. (ξ, η) . For the computation of $\epsilon_{\delta\theta_c}$ and ϵ_A , we assume a point source. For the discussion about the finite-size source effect, see § 6 of Gaudi & Gould (1997). In Figure 3, we present the contours of excess centroid shift for events with various binary separations and mass ratios $q = m_1/m_2$ between the binary components. In the figure, contours are drawn at the levels of $\epsilon_{\delta\theta_c} = 0.30$ (thickest lines), 0.10, and 0.03 (lightest lines). The contours of excess amplification for events with the same binary separations and mass ratios are found in Figure 1 of Gaudi & Gould (1997), in which the contours are drawn at the levels of $\epsilon_A = \pm 0.10$ and ± 0.03 . One finds that the region of significant centroid shift deviation is much larger than the region of amplification deviation measured at the same level of excess. In Figure 4, we also present contours of excess centroid shifts for binaries with very small separation ($b \leq 0.1r_E$). From the figure, one finds that the regions of noticeable excess centroid shift is considerable even for very small values of b .

Once the contours of excess amplification and centroid shift are constructed, the binary detection rates are obtained by computing the ratio of the number of events whose source locations are within the excess region during the measurements to the total number of trial events. The source trajectory orientations with respect to the projected binary axis, θ , and the impact parameters, β , are randomly chosen in the ranges of $0 \leq \theta \leq 2\pi$ and $0 \leq \beta \leq 1$. Measurements for each event is assumed to be performed 25 times during the event, which corresponds to one measurement per day for a Galactic bulge event caused by a total mass of $M \sim 0.4 M_\odot$ (Gaudi & Gould 1997). We consider a binary to be detected if the excess is greater than some threshold excess values: ϵ_A and $\epsilon_{\delta\theta_c}$ for photometric and astrometric measurements respectively. Following Gaudi & Gould (1990), we adopt the two threshold values of 0.03 and 0.1.

Figure 4 shows the binary detection rates as a function of binary separation and mass ratio expected from the photometric and astrometric observations of microlensing events. To better show the detection rates for binaries with very small separations and mass ratios, we present the values of b and q on a logarithmic scale. Contours have equal spacing of 10% and the threshold excess amplification and centroid shift are marked in each panel. From the comparison of detection rates between the two methods, one finds that the astrometric detection rates are significantly larger than the photometric rates in all regions of b - q space. For example, while the photometric detection rates for a binary lens with $(b, q) = (0.3, 0.1)$ are $\Gamma_{\text{ph}} < 10\%$ and $\sim 15\%$ with the threshold excesses of $\epsilon_A = 0.1$ and 0.03 respectively, the astrometric detection rates for the same binary are $\Gamma_{\text{ast}} \sim 70\%$ and $\sim 95\%$ with the same thresholds. Our proposed method is especially efficient at detecting very close binaries. With a detection threshold of $\epsilon_{\text{as}} = 0.03$ and a rate of 10%, one can astrometrically detect binaries with separations down to $\sim 0.01r_E$.

4. Summary

Gravitational microlensing provides us with an important method of constructing the Galactic matter mass function which is free from the biases induced by the hydrogen burning limit. In addition, by detecting the deviations in light curves due to binary systems, one can construct a mass function that is less affected by the problem of unresolved binaries. However, since the light curves of binary-lens events with very small separations mimic those of single-lens events, the photometric detection of binaries is limited to systems with relatively large binary separations. Therefore, although photometric microlensing observations provide a superior method of detecting binaries, the constructed mass function will not be totally free from the problem of unresolved binaries. However, by astrometrically measuring the distortions of astrometric ellipses, one can not only significantly improve the binary detection rate but also detect binaries with much smaller separations. Therefore, astrometric observations of microlensing events can significantly reduce the uncertainties in the mass function caused by unresolved binaries.

We would like to thank to P. Martini and M. Everett for careful reading the manuscript. We also would like to thank B. S. Gaudi & A. Gould for kindly providing a program to compute amplifications of binary-lens events. Chang, K. was supported by a Korean Science and Engineering Foundation (KOSEF) grant 971-0203-012-2.

REFERENCES

- Alard, C., & Guibert, J. 1997, A&A, 326, 1
- Alcock, C., et al. 1997a, ApJ, 479, 119
- Alcock, C., et al. 1997b, ApJ, 486, 697
- Ansari, R., et al. 1996, A&A, 314, 94
- Ansari, R., et al. 1997, A&A, 324, 843
- Boden, A. F., Shao, M., & Van Buren, D. 1998, ApJ, 502, 538
- Crotts, A. P. S. 1992, ApJ, 399, L43
- Dominik, M. 1998, A&A, 329, 361
- Gaudi, B. S., & Gould, A. 1997, ApJ, 482, 83
- Gould, A. 1996, PASP, 108, 465
- Han, C., & Gould, A. 1996, ApJ, 467, 540
- Han, C., & Chang, K. 1998, MNRAS, 299, 1040
- Han, C., & Jeong, Y. 1998, MNRAS, 301, 231
- Jeong, Y., Han, C., & Park, S.-H. 1999, ApJ, 511, 569
- Jetzer, Ph. 1994, ApJ, 432, L43
- Kroupa, P., Tout, C., & Gilmore, G. 1991, MNRAS, 251, 293
- Mao, S., & Paczyński, B. 1991, ApJ, 374, L37
- Paczynski, B. 1998, ApJ, 404, L23
- Reid, N. 1991, AJ, 102, 1428
- Safizadeh, N., Dalal, N., & Griest, K. 1998, preprint (astro-ph/9811233)
- Schneider, P., & Weiss, A. 1986, A&A, 164, 237
- Tomaney, A. B., & Crotts, A. P. S. 1996, AJ, 112, 2872
- Udalski, A. et al. 1997, Acta Astron. 47, 169
- Walker, M. A. 1995, ApJ, 453, 37
- Zhao, H., Rich, R. M., & Spergel, D. N. 1996, MNRAS, 282, 175
- Witt, H. 1990, A&A, 263, 311

Figure 1: The geometry of gravitational microlensing for various binary lens separations. In the figure, the two lenses with equal masses are located on the ξ -axis (indicated by two dots) and the separation b between them is marked in each panel. The closed figures drawn with dotted and thick solid lines represent critical curves and caustics, respectively. For events with $b = 0.1$ and $b = 0.4$, there exist two additional triangular caustics outside the regions shown. In addition, there are two small circular critical curves near the diamond-shaped central caustic, but they are too small to be seen in the figure. The arclets drawn with a thin solid line represent the images of the source star, which is located at $(\xi, \eta) = (-0.3, -0.32)$ and is marked by a shaded circle. The source star is assumed to have a radius of $0.05r_E$. When the source star is located outside the caustics as shown in the figure, there exist three images. However, the smallest image inside the central caustic for small b is too small to be seen. The straight lines in the panel for $b = 0.1$ represent the source star trajectories which are responsible for the astrometric shifts and light curves in Figure 2.

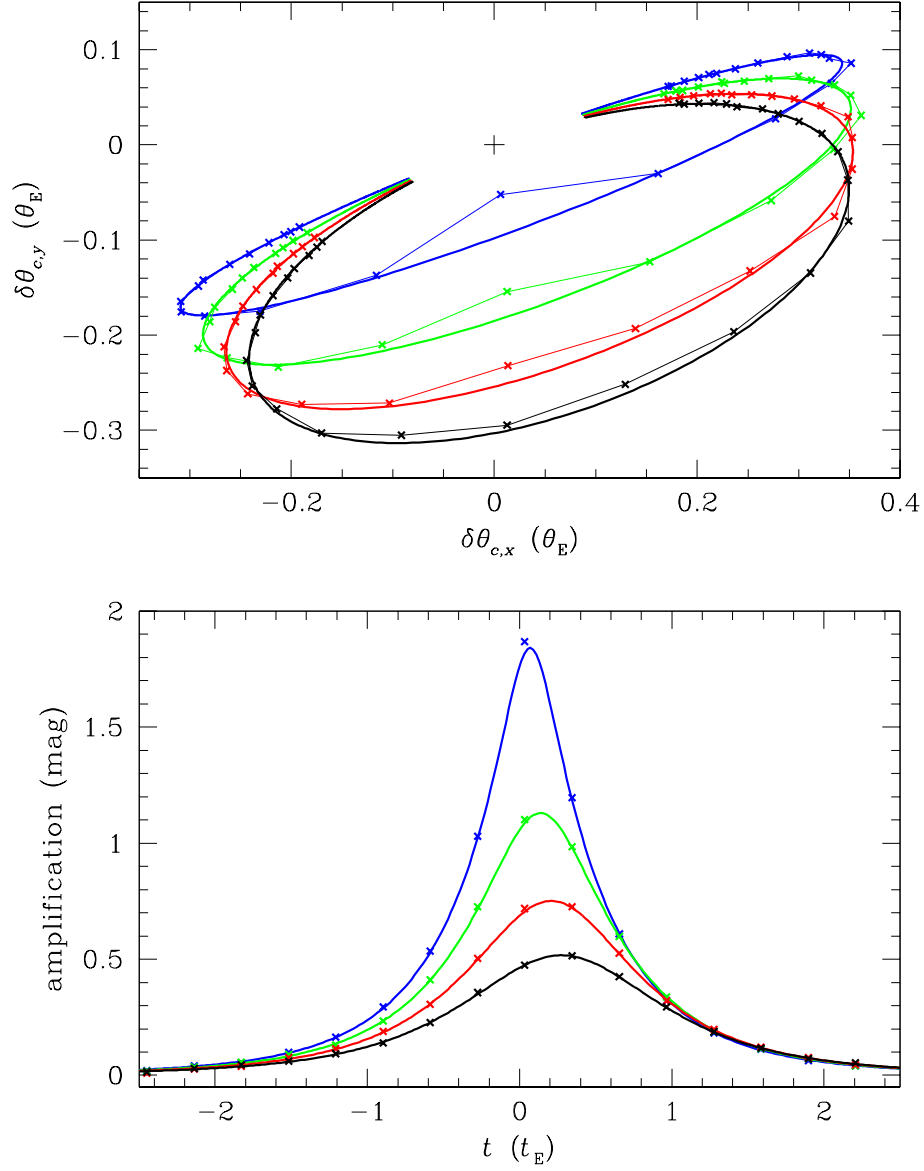


Figure 2: The astrometric light centroid shifts and light curves of close binary-lens events. The centroid shifts and light curves are for the binary-lens event in the upper left panel of Figure 1, in which the corresponding source star trajectories are marked by straight lines. The ‘x’ symbols mark the centroid shifts and amplifications for the binary-lens event, while the smooth solid curves are for a single-lens event with a mass equal to the total mass of the binary and located at the center of mass of the binary.

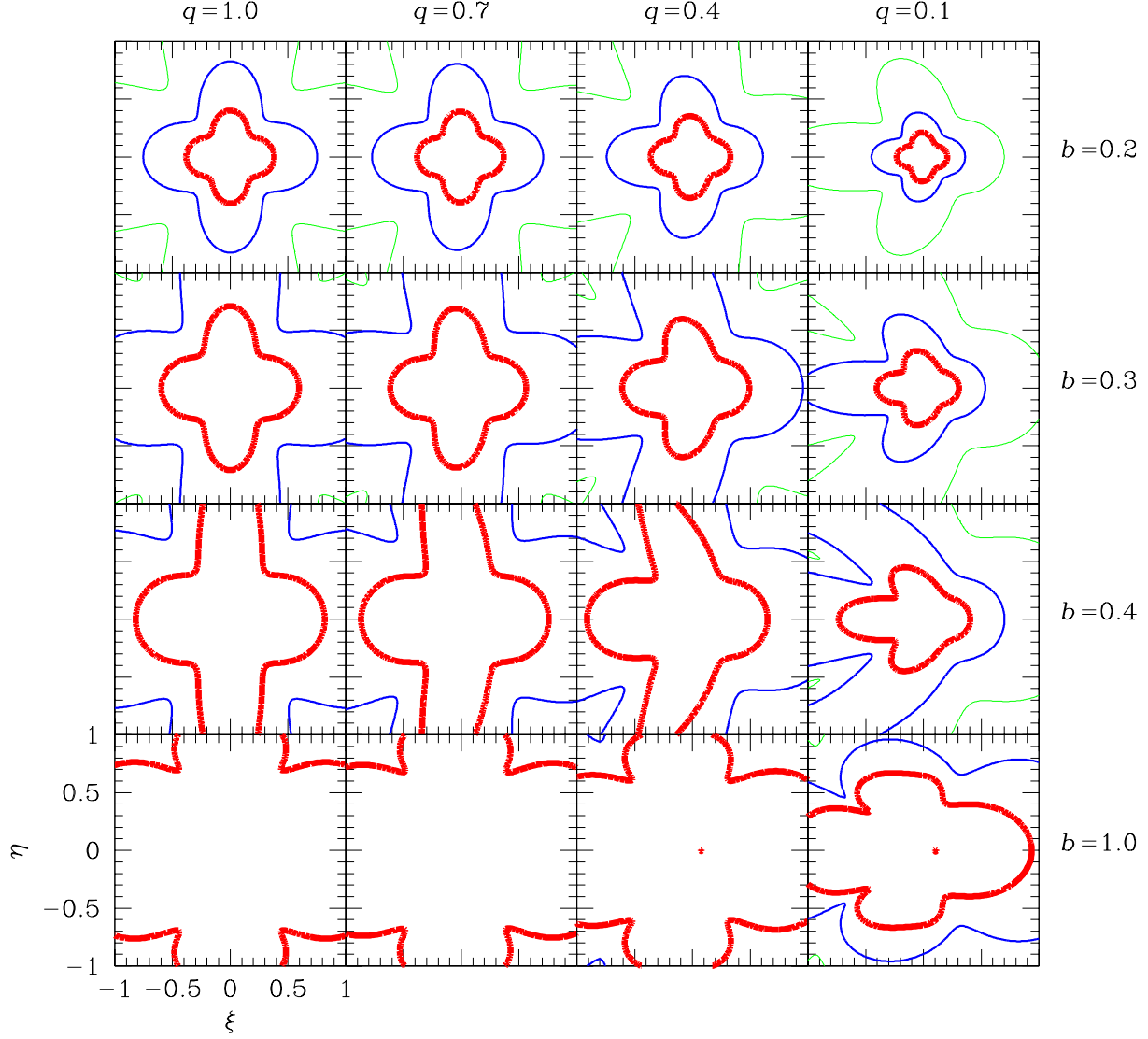


Figure 3: Contours of excess centroid shift, $\epsilon_{\delta\theta_c}$, for events with various binary separations and the mass ratios between the binary components. Contours are drawn at the levels of $\epsilon_{\delta\theta_c} = 0.30$ (thickest lines), 0.10, and 0.03 (lightest lines). The positions of the masses are chosen so that the center of mass is at the origin, but both masses are on the ξ -axis, and the smaller mass is to the left. For direct comparison with the contours of excess amplification of Gaudi & Gould (1997), we choose the same positions of masses, binary separations, and binary-component mass ratios.

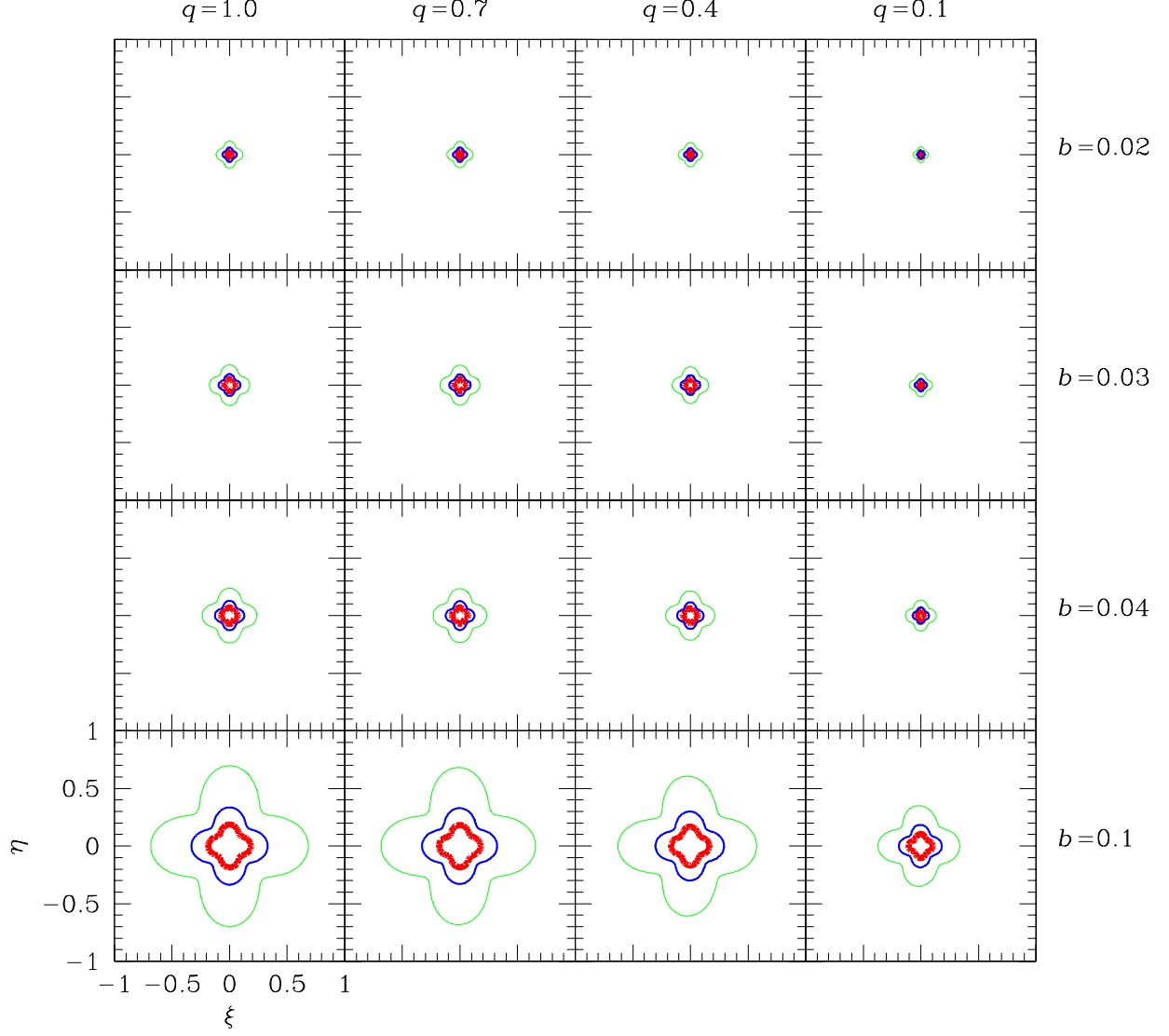


Figure 4: Contours of excess centroid shift, $\epsilon_{\delta\theta_c}$, for binary-lens events with very close binary separations. The positions of the masses and the levels of the contours are chosen in the same way as in Figure 3.

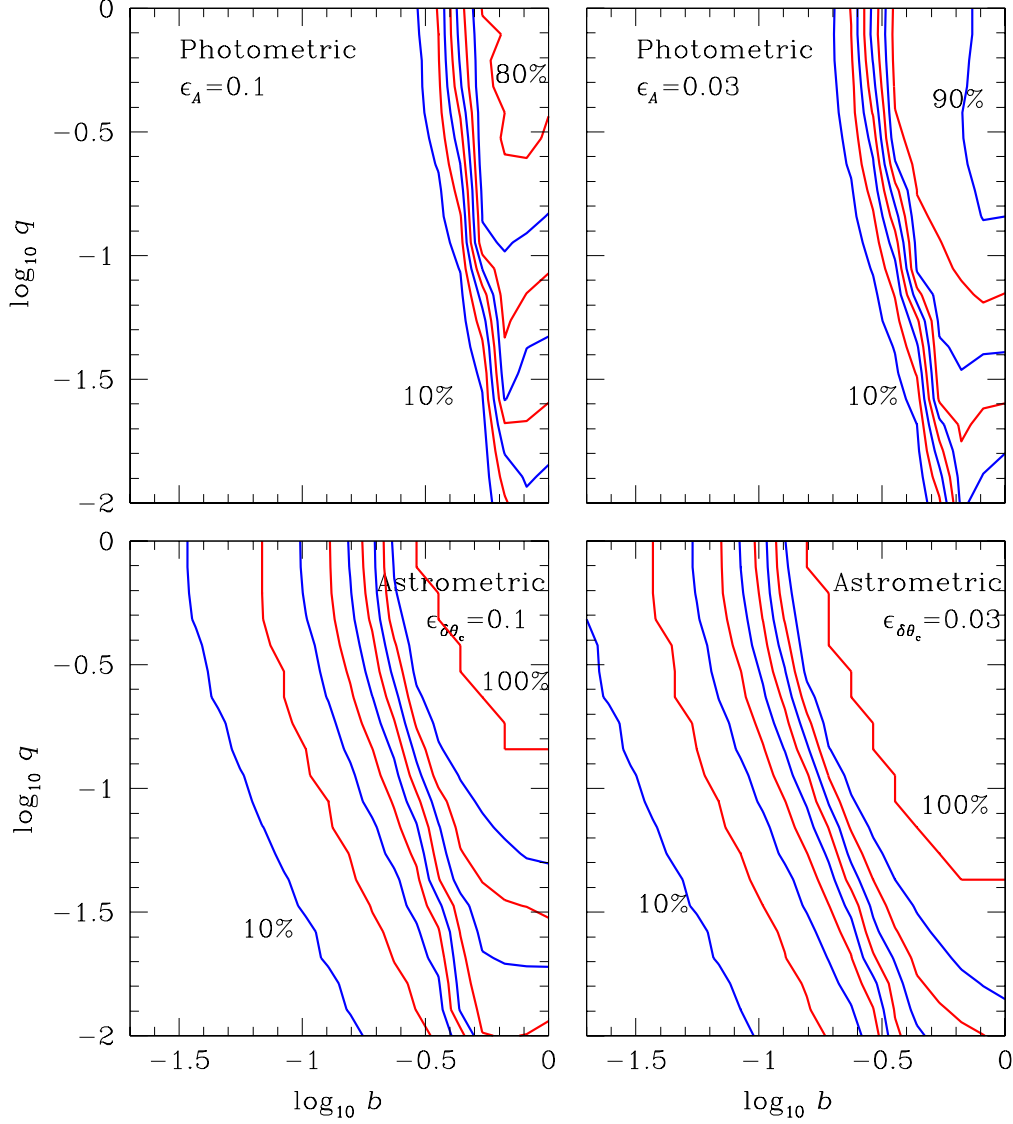


Figure 5: Binary detection rates as a function of binary separation and mass ratio expected from the photometric and astrometric observations of microlensing events. Contours have equal spacing of 10%. To better show the event rates for binaries with very small separations and mass ratios, the values of b and q are presented in logarithmic scale. A binary is considered to be detected if the excess of amplification (and the centroid shift) is greater than the threshold value (marked in each panel) during the measurements.